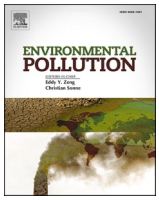
Environmental Pollution 363 (2024) 125114



Contents lists available at ScienceDirect

Environmental Pollution

journal homepage: www.elsevier.com/locate/envpol





Inter-annual changes in transboundary air quality from KORUS-AQ 2016 to SIJAQ 2022 campaign periods and assessment of emission reduction strategies in Northeast Asia☆

Min-Jun Park [a], Seung-Hee Baek [a], Hyo-Jung Lee [a,b,*], Hyun-Young Jo [b,**], Cheol-Hee Kim [a,b], Jin-Seok Kim [c,d], Jung-Hun Woo [e], Rokjin Park [f], Jong-Jae Lee [g,h,i], Chang-Keun Song [g,h,i], Jung-Woo Yoo [b], Lim-Seok Chang [j], Taehyoung Lee [k]

[a] Department of Atmospheric Sciences, Pusan National University, Busan, 46241, Republic of Korea
[b] Institute of Environmental Studies, Pusan National University, Busan, 46241, Republic of Korea
[c] Department of Advanced Technology Fusion, Konkuk University, Seoul, 05029, Republic of Korea
[d] Environmental Planning Institute, Seoul National University, Seoul, 08826, Republic of Korea
[e] Graduate School of Environmental Studies, Seoul National University, Seoul, 08826, Republic of Korea
[f] School of Earth and Environmental Sciences, Seoul National University, Seoul, 08826, Republic of Korea
[g] Department of Civil Urban Earth and Environmental Engineering, Ulsan National Institute of Science and Technology (UNIST), Ulsan, 44919, Republic of Korea
[h] Graduate School of Carbon Neutrality, Ulsan National Institute of Science and Technology (UNIST), Ulsan, 44919, Republic of Korea
[i] Research & Management Center for Particulate Matters at the Southeast Region of Korea, Ulsan National Institute of Science and Technology (UNIST), Ulsan, 44919, Republic of Korea
[j] Environmental Satellite Center, National Institute of Environmental Research, Incheon, 22689, Republic of Korea
[k] National Department of Environmental Science, Hankuk University of Foreign Studies, Yongin, 17035, Republic of Korea

ARTICLE INFO

Keywords:
Long-range transport
$PM_{2.5}$
Secondary inorganic aerosol (SIA)
Chemical transformation
Gas-to-particle conversion
WRF-Chem

ABSTRACT

Northeast Asia suffers from high concentrations of particulate matter (PM), prompting nations to actively implement emission reduction policies. This study evaluated the recent inter-annual changes in the chemical transformation and transboundary transport of PM over Northeast Asia, based on both ground and aircraft measurements, as well as WRF-Chem simulations, during two comprehensive campaigns: the Korea–United States Air Quality (KORUS-AQ) campaign in 2016 and the Satellite Integrated Joint Monitoring of Air Quality (SIJAQ) campaign in 2022, both conducted around the Korean Peninsula. Ground measurements in 2022 revealed significant reductions in air pollutants compared to 2016 levels. In the Beijing–Tianjin–Hebei region, $PM_{2.5}$ and SO_2 concentrations decreased by 47.2% and 73.9%, respectively, attributable to successful SO_x and NO_x emission reduction strategies. Similar trends were observed in downwind areas, including Seoul, where $PM_{2.5}$ and SO_2 levels declined by 30.0% and 41.4%, respectively. WRF-Chem model results indicated substantial decreases in sulfates, nitrates, and their precursors in both surface and upper atmosphere in 2022 compared to 2016. Moreover, model-calculated gas-to-particle conversion ratios, which peaked in the Yellow Sea in 2016, decreased by 15% in 2022 and shifted slightly eastward to the western Korean Peninsula. This shift suggests a potential decline in secondary PM formation processed in the Yellow Sea, coinciding with reduced long-range transport of gaseous pollutants. A comparison of model sensitivity experiments, accounting for both bottom-up emission changes and meteorological variations, revealed that while weather and climate factors such as precipitation and pressure patterns between 2016 and 2022 contributed to the overall decrease in PM concentrations, the primary driver was the reduction in emissions during this period. This study highlighted that the main driver of the substantial improvement in air quality over East Asia was the implementation of emission reduction policies targeting PM and its precursors in the main source regions in China.

☆ This paper has been recommended for acceptance by Pavlos Kassomenos.

* Corresponding author. Department of Atmospheric Sciences, Pusan National University, Busan, 46241, Republic of Korea.
** Corresponding author.
E-mail address: hyojung@pusan.ac.kr (H.-J. Lee).

https://doi.org/10.1016/j.envpol.2024.125114
Received 16 July 2024; Received in revised form 6 October 2024; Accepted 11 October 2024
Available online 12 October 2024
0269-7491/© 2024 Elsevier Ltd. All rights are reserved, including those for text and data mining, AI training, and similar technologies.

1. Introduction

Northeast Asia's rapid economic growth has been accompanied by a significant increase in air pollution over the past few decades, posing a serious threat to public health and the environment (Matus et al., 2012; WHO, 2013; Fuzzi et al., 2015; He et al., 2017). Recognizing the urgency of this issue, East Asian countries have implemented various emission reduction policies designed to mitigate the adverse effects of air pollution related to high $PM_{2.5}$ levels. Since 2003, the Korean government has been steadily executing regulatory policies, starting with the Special Act on Air Quality in the Seoul Metropolitan Area (Kim and Lee, 2018). The Japanese national and local governments have been endeavoring to improve air quality by imposing environmental policies to address severe industrial pollution since the 1960s and 1970s (Hamamoto, 2006; Itawa et al., 2014). In China, the government has been implementing robust emission reduction policies under its air pollution prevention and control strategy since 2000s. The Air Pollution Prevention and Control Action Plan (APPCAP), introduced in 2013, established targets for particulate matter (PM) reduction across China and in key regions through 2017 (Feng et al., 2019; Wu et al., 2017). The subsequent Three-Year Action Plan for Winning the Blue Sky Defense Battle (the Three-Year Action Plan; the second phase) from 2018 to 2020 significantly improved air quality in China (Lu et al., 2020; Zheng et al., 2022). Most recently, China's 14th Five-Year Plan (14th-FYP Action Plan), representing the third phase of its comprehensive air pollution control strategy, has set an ambitious target to further reduce the annual mean $PM_{2.5}$ concentration by 10% between 2020 and 2025 (Zheng et al., 2022; Cheng et al., 2024). This sequential implementation of stringent air quality policies demonstrates China's sustained efforts for addressing air pollution at both national and regional scales.

Since the implementation of recent emission reduction policies, numerous diagnostic studies have been conducted using intensive measurement data and comprehensive modeling on changes in air pollutant concentrations (Wang et al., 2014; Guo et al., 2016). Many previous studies on changes in the occurrence of severe haze in China due to emission reduction have been pivotal in understanding the physicochemical mechanisms of changes in $PM_{2.5}$ production from its precursors (Zhang et al., 2018; Peterson et al., 2019; Jo et al., 2022). Consequently, SO_2, NO_x, and $PM_{2.5}$ concentrations have decreased remarkably (Gao et al., 2020; Lu et al., 2020). The concentrations of secondary inorganic aerosols, such as sulfate, nitrate, and ammonium, and secondary organic aerosols have also changed (Sun et al., 2016).

With the main emission source regions on the upwind side of Northeast Asia, the recent notable emissions shifts can significantly affect the air quality of downstream areas via transboundary transport process over Northeast Asia. Numerous researchers have investigated the variations of air quality characteristics over South Korea and Japan in response to changes in emissions in China (Kaneyasu et al., 2014; Jo et al., 2020; Han et al., 2021; Xia et al., 2016; Lee et al., 2021, 2022; Xie and Liao, 2022). Xie and Liao (2022) used the global atmospheric chemistry model GEOS-Chem to examine the effect of China's anthropogenic emission changes on $PM_{2.5}$ concentrations in South Korea and Japan from 2013 to 2017. The study reported that the reduction in China's anthropogenic emissions alone led to decreases in annual average $PM_{2.5}$ concentrations of 13.7 (19.7%), 2.7 (7.7%), and 1.0 (7.9%) in East China, South Korea, and Japan, respectively. Han et al. (2021) utilized the regional air quality model RAMS-CMAQ coupled with integrated source partition to analyze quantitatively the contribution of China's emission changes to $PM_{2.5}$ concentrations in Korean Peninsula. The results revealed that the annual average contribution of China's emissions to $PM_{2.5}$ concentrations in the Korean Peninsula decreased significantly from 28.0% in 2010 to 15.7% in 2017, further substantiating the effectiveness of China's air pollution management.

Most of these previous studies focused on evaluating average changes in $PM_{2.5}$ mass concentrations and chemical components in the Korean Peninsula due to variations in emissions from China. However, research is limited about the quantitative assessment of impact of emission reduction in China on the long-range transport and consequent concentration of air pollutants in its downwind areas. Jo et al. (2020) reported a decrease in sulfate in downwind areas due to changes in China's emissions in 2014–2016, focusing on Baengnyeong Island, an entry area for long-range transport, using Weather Research and Forecasting regional air quality and chemistry model (WRF-Chem) simulations and observational data. However, they indicated that three-dimensional (3D) observational data from satellites and aircraft are required for a more comprehensive understanding of the spatial distribution patterns and migration paths of fine particles.

In this study, we aimed to investigate the air quality characteristics and related chemical formation processes in downwind areas influenced by China's reduced emissions using various data from campaigns conducted on the Korean Peninsula. Specifically, we used diverse ground and aircraft data measured during the Korea–United States Air Quality (KORUS-AQ) campaign (May–June 2016) (Crawford et al., 2021) and the Satellite Integrated Joint Monitoring of Air Quality (SIJAQ) 2022 campaign (May–June 2022) together with WRF-Chem results. We also examined changes in long-range air pollutant transport and secondary formation processes over Northeast Asia.

2. Material and methods

2.1. Study period

Intensive aircraft and field campaigns have been conducted in the Korean Peninsula to understand the precursor emissions, transport pathways, and chemical mechanisms of air quality in South Korea. First, the KORUS-AQ campaign was conducted from May to June 2016 by the National Institute of Environmental Research (NIER) in South Korea and the National Aeronautics and Space Administration (NASA) in the United States. During the campaign, trace gases, aerosol particle properties, and meteorological variables were measured using a DC-8 aircraft, ground sites, and ships to obtain a multi-perspective view of air quality conditions over South Korea. Subsequent campaigns have been performed in East Asia for the validation of operating the geostationary environment monitoring spectrometer (GEMS) retrievals: the GEMS Map of Air Pollution (GMAP) campaign in 2020 and the SIJAQ campaigns in October–November 2021 and May–June 2022.

This study examined trends in ground-measured air pollutant concentrations across upwind and downwind regions from 2016 to 2022, with a particular emphasis on the effects of emission reduction measures in China. Throughout our analysis, we refer to this 7-year variation as the "inter-annual change of air pollutants". Our study incorporated an in-depth analysis of aircraft measurements and model simulations, specifically concentrating on the two campaign periods: May–June 2016 (KORUS-AQ, 2016) and May–June 2022 (SIJAQ 2022). These campaigns, conducted during the same seasonal period but in different years, served as a case studies to examine the physicochemical changes in air quality across East Asia resulting from China's emission reduction strategies between 2016 and 2022.

2.2. Data

2.2.1. In situ observation

The inter-annual variabilities in air quality due to emission reductions in China were analyzed using the long-term (2016–2022) trends of the surface concentrations of air pollutants in upwind and downwind areas. We used hourly average concentration data of $PM_{2.5}$, SO_2, NO_2, CO, and O_3 from the China National Environmental Monitoring Center for the upwind area and the Urban Monitoring Network operated by the NIER in South Korea for the downwind areas. These datasets are publicly accessible through the official websites: https://www.cnemc.cn for China and https://www.airkorea.or.kr for South Korea. Detailed information regarding data quality assurance and

quality control procedures for each data is available on the respective websites. The measurement data from the upwind area were pollutant concentrations at 147 sites in the Beijing–Tianjin–Hebei (BTH) region, China (115°–117.5° E, 38.5°–41° N). The measurements in the downwind areas were from 25 measurement sites in Seoul (typical urban site) and Baengnyeong Island (background site), South Korea (Fig. 1). We excluded periods of Asian dust events to enhance the reliability of the results on the secondary formation of PM from the measurement data.

In this study, meteorological variables derived from WRF-Chem simulations for the KORUS-AQ 2016; SIJAQ 2022 periods were evaluated and compared against observations. For Seoul and Baengnyeong Island, data from the Korea Meteorological Administration's (KMA) Automated Surface Observing System (ASOS) were used. For Beijing, data from the Global Telecommunication System (GTS) were utilized.

2.2.2. Campaign measurements

We used aircraft measurement data from the KORUS-AQ 2016; SIJAQ 2022 campaigns. During the KORUS-AQ campaign (May–June 2016), a total of 20 flight measurements were conducted by DC-8, targeting the areas of the Yellow Sea and South Korea. Each measurement included various substances such as gaseous air pollutants (SO_2, NO_x, CO, and O_3) and particulate air pollutants (SO_4^{2-}, NO_3^-, NH_4^+, black carbon, and organic aerosols), with data collected over approximately 4–8 h (NIER and NASA, 2017; Crawford et al., 2021). The KORUS-AQ 2016 campaign data are available through the NASA Langley Research Center archive at https://www-air.larc.nasa.gov/cgi-bin/ArcView/korusaq. The quality assurance (QA) and quality control (QC) procedures for airborne observations, as well as detailed specifications of the instruments used for measuring each chemical species, are available on the aforementioned website and in Crawford et al. (2021).

The SIJAQ 2022 performed a total of 35 measurements with each measurement lasting approximately 3–4 h and targeting the Yellow Sea region. The measured chemical components were NO_2, O_3, CO, and various types of volatile organic compounds. SIJAQ 2022 campaign data are accessible at https://www.sijaq.org, which also provides details on measurement instruments and QA/QC processes, analogous to those for the KORUS-AQ airborne measurements, can also be found. The SIJAQ 2022 airborne measurement data, lacking PM composition, were solely used to evaluate the accuracy of WRF-Chem simulations for vertical structures of gaseous air pollutants.

To address the absence of PM components from the SIJAQ 2022 airborne measurements and to analyze trends in PM components, we utilized ground-based PM component concentrations collected at Olympic Park (127.121° E, 37.520° N) in central Seoul during both the SIJAQ 2022; KORUS-AQ 2016 campaigns. Hourly concentrations of $PM_{2.5}$ chemical components (NO_3^-, SO_4^{2-}, and NH_4^+) measured at the surface during each campaign period were obtained from the respective campaign websites. These ground and airborne measurements, combined with atmospheric chemical transport model results, were employed to examine inter-annual changes in transboundary transport processes by comparing gaseous and particulate pollutant profiles between the SIJAQ 2022; KORUS-AQ 2016 campaign periods.

2.2.3. Aerosol optical depth (AOD) data: VIIRS and MEERA-2

To examine the variations in PM concentrations across Northeast Asia due to China's emission reductions, we used aerosol optical depth (AOD) data from the Visible Infrared Imaging Radiometer Suite (VIIRS) on the Suomi-NPP satellite and the Modern-Era Retrospective Analysis for Research and Applications, version 2 (MERRA-2), along with ground measurement data. The MERRA-2 data were obtained from NASA's Global Modeling and Assimilation Office (Geralo et al., 2017). VIIRS Level-3 data with horizontal resolution of 1° × 1° were utilized to extract and analyze Aerosol Optical Depth (550 nm) for the two campaign periods. Additionally, to analyze the AOD over East Asia, reanalysis data were used in conjunction with satellite observation data. The horizontal resolution of the MERRA-2 data was 0.5° × 0.625°, and we extracted and analyzed the total aerosol extinction AOD (550 nm) variable during the spring season, which covered the two campaign periods in 2016 and 2022. The VIIRS and MERRA-2 AOD data were also used to verify the model's simulation capability of PM spatial distributions by comparing its findings with simulated $PM_{2.5}$ columns over Northeast Asia.

2.3. Model configuration and emissions

2.3.1. Emissions

Emission data sets from bottom-up emission calculations corresponding to each period (2016 and 2022) were used: the updated Comprehensive Regional Emissions for Atmospheric Transport Experiment, version 3 (CREATEv3) for SIJAQ 2022 and the latest anthropogenic KORUS-AQ emission inventory (KORUSv5) for KORUS-AQ 2016. Both data sets were verified in previous studies on the characteristics of air qualities for both campaigns (Park et al., 2021; Kim et al., 2023a).

The emission data for KORUS-AQ 2016 were obtained from

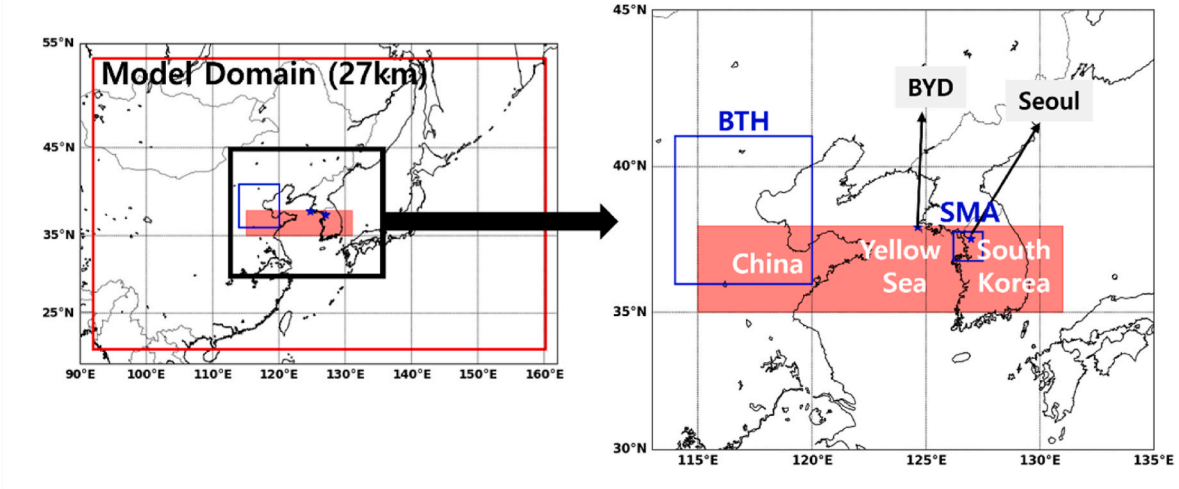


Fig. 1. Modeling domains and locations of study area: Beijing–Tianjin–Hebei (BTH), Yellow Sea, and Korean Peninsula. The red squares indicate the area used in the curtain plot to analyze the vertical structure of pollutants in this study. (For interpretation of the references to colour in this figure legend, the reader is referred to the Web version of this article.)

KORUSv5, which is originally a combination of inventories from 29 Asian countries, including the Regional Emission Inventory in Asia, Multiresolution Emission Inventory China (MEIC), Japan Auto-Oil Program Emission Inventory, and Korean Clear Air Policy Support System (CAPSS). The emission data for SIJAQ 2022 were the updated CREATEv3 product, which is also from a combination of inventories (MEIC for China's emissions and CAPSS for Korea's emissions) (Kim et al., 2023b). The Model of Emissions of Gases and Aerosols from Nature (MEGAN), version 2.04, was used for biogenic emissions for both KORUS-AQ 2016; SIJAQ 2022. These emission inventories were described in detail by Woo et al. (2020).

2.3.2. Model configuration

We used the 3D mesoscale photochemical transport model WRF-Chem (version 3.9.1) (Skamarock and Klemp, 2008; Grell et al., 2005) and numerically simulated the air pollutants during the KORUS-AQ 2016; SIJAQ 2022 campaign periods, including $PM_{2.5}$, SO_2, NO_2, and NH_3. WRF-Chem is configured with a horizontal resolution of 27 km (174 × 126 grids) and a vertical resolution of 28 layers (Fig. 1). This domain setup was replicated as in the model configuration used in previous model intercomparison studies (Park et al., 2021; Gao et al., 2020) that investigated air pollutant behavior in East Asia. The initial and boundary meteorological conditions were from National Centers for Environmental Prediction (NCEP) Final Analysis (FNL) data, which have a time resolution of 6 h intervals and a horizontal spatial resolution of 1° × 1° (NCEP, 2000).

As for chemical gas and aerosol schemes, we used the Earth System Research Laboratories (ESRL) regional atmospheric chemistry model (RACM) as the gas-phase chemical scheme, and the modal aerosol dynamics model for Europe–volatility basis set (MADE/VBS) as the aerosol scheme. The detailed physical and chemical process settings in the model are summarized in Table S1.

The WRF-Chem model settings for the KORUS-AQ 2016 are identical to those for the SIJAQ 2022 except the base year of simulation and anthropogenic emission data (Lee et al., 2023). Using the configuration of the WRF-Chem simulations, we made a comparative analysis of the simulation results and examined the differences in air quality over the Korean Peninsula arising from China's emission reduction strategies during the two campaign periods.

3. Results and discussion

3.1. Interannual changes in surface concentrations and emissions

Fig. 2 illustrates the 7-year trends of the monthly averages of several air pollutants from ground measurements over seven years in both upwind area (BTH, China) and downwind areas (Seoul and Baengnyeong Island, South Korea). In the upwind region (China), the SO_2, NO_2, and $PM_{2.5}$ concentrations substantially decreased, which was attributable to the strong implementation of China's emission reduction policies between 2008 and 2020 (Liu et al., 2020). In previous studies, these policies reduced the levels of precursor gases and PM (Chen et al., 2019; Shi et al., 2021). Our study showed that, in the BTH area, the concentrations of most air pollutants declined, with an approximately 1.5 ppbv/year reduction in SO_2, 1.6 ppbv/year in NO_2, and 5.6 μg/m^3/year in $PM_{2.5}$ levels in 2016–2022. In the downwind regions, Seoul exhibited annual decreases of approximately 0.3 ppbv/year in SO_2 concentrations and 5%/year in $PM_{2.5}$ concentrations. Baengnyeong Island, located in the Yellow Sea (Fig. 2) and reflecting the background concentration of the Korean Peninsula, also exhibited a notable decrease in SO_2 (0.2 ppbv/year) and marginal decreases in $PM_{2.5}$ (0.7 μg/m^3/year). This study hypothesized that these decreases in air pollutants on Baengnyeong Island were attributable to China's emission reduction, considering its geographical proximity to China and the prevailing westerly wind patterns in spring, and the sites in Seoul are influenced by their own plus foreign pollutant emissions. Given the hypothesis above, the more pronounced decrease in SO_2 concentrations in these sites could thus be attributed to South Korea's emission reduction as well as emission reduction in upwind areas.

We quantitatively assessed our hypothesis: the effects of reduction of anthropogenic emissions on the levels of air pollutants in each region by comparing the spatial bottom-up emission in the two campaign periods: KORUS-AQ 2016; Park et al. (2021); SIJAQ 2022; Kim et al. (2023a); Park et al. (2024). Fig. 3 shows two bottom-up emission distributions and total reduction in emission in each campaign period. In most areas in the BTH region (115.0°–117.5° E, 38.5°–41.0° N), East China, the SIJAQ 2022 campaign emissions showed reductions in all gaseous and particulate air pollutants, such as NH_3, NO_2, SO_2, and primary $PM_{2.5}$, compared with the KORUS-AQ 2016 campaign emissions. Total reduction in South Korea showed relatively smaller SO_2 and NO_2 emission reductions, which were 38.8 and 3.4 ton/km^2, respectively, compared with East China, which exhibited reductions of 335.3 and 16.3 ton/km^2/h, respectively. The reduction rates during the two campaign periods showed that SO_2 emissions were reduced by approximately 71%, NH_3 by 51%, NO_2 by 28%, and primary $PM_{2.5}$ by 37% in East China. These results were well consistent with the annual reduction rates in NO_x and SO_2 emissions (17% and 62%, respectively) from 2010 to 2017 in previous studies in China (Zheng et al., 2018; Zeng et al., 2019). South Korea exhibited a similar annual SO_2 emission reduction (72%) to that of East China, but its decreases in the other species were lower than those of East China. Accordingly, Korea's air quality might have been affected more by China's emission reduction. South Korea's

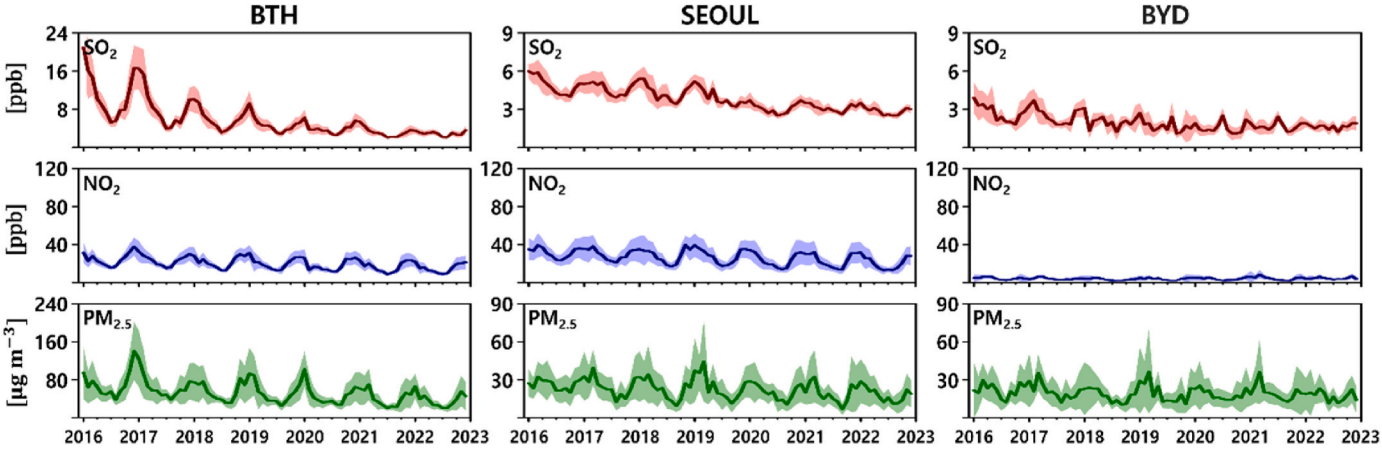


Fig. 2. Changes in monthly average levels of observed SO_2, NO_2, and $PM_{2.5}$ in China's BTH region (115.0°–117.5° E, 38.5°–41.0° N) and Korean Peninsula's Seoul (126.83°–127.14° E, 37.48°–37.66° N) and Baengnyeong Island (BYD; 124.63° E, 37.96° N) in 2016–2022.

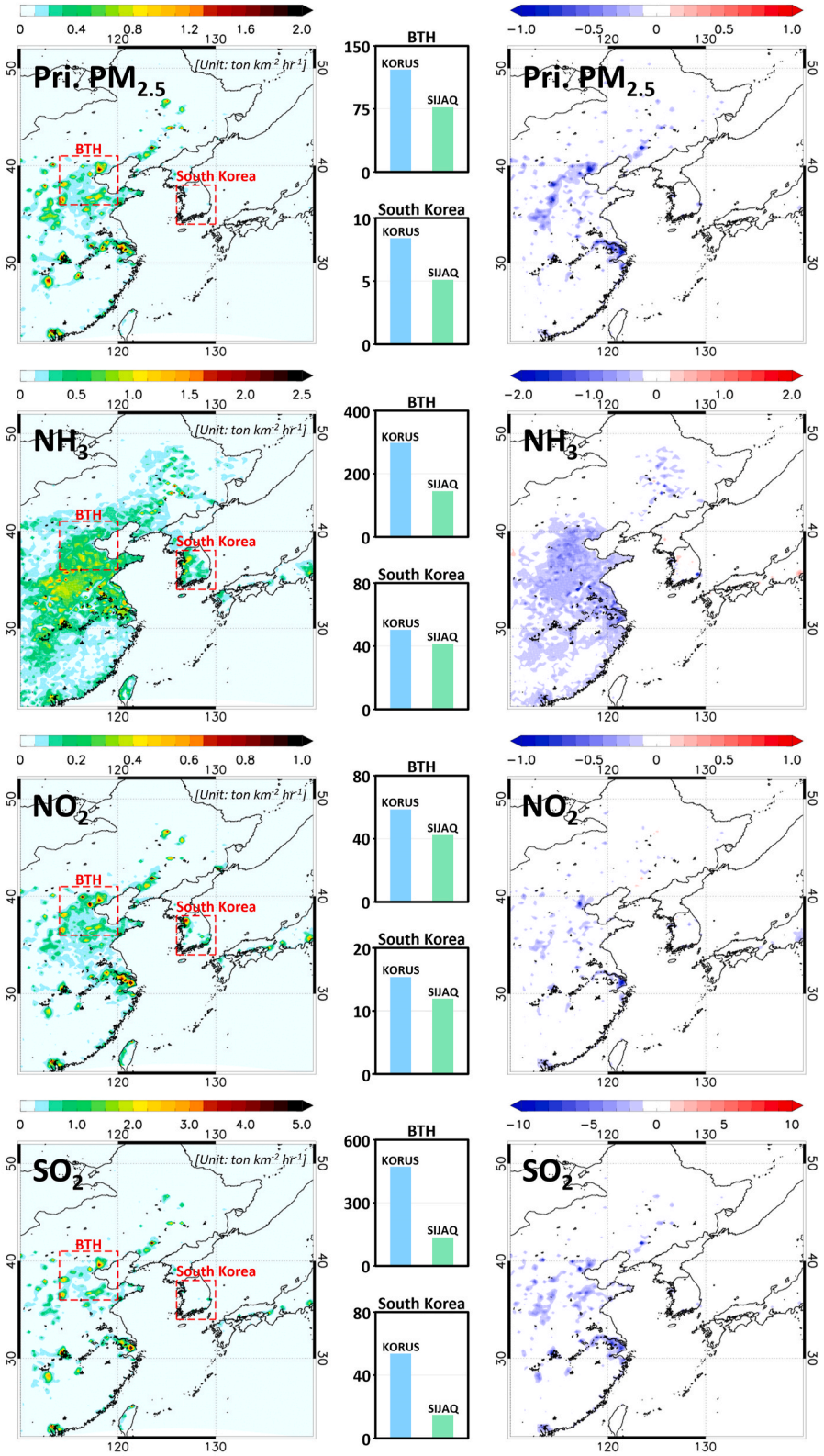


Fig. 3. Comparisons of spatial distributions and total emissions (ton km^2 hr^{-1}) of bottom-up estimates. Emissions during SIJAQ 2022 (left), for the BTH region and South Korea (mid), and differences between the SIJAQ 2022; KORUS-AQ 2016 periods (right).

domestic reduction efforts may have had some impact, but it was relatively low. Therefore, we conducted several sensitivity tests to verify this hypothesis using the WRF-Chem atmospheric chemistry model and aircraft measurements. We also identified the changes in the potential effects of the transboundary transport of high-concentration pollutants over Northeast Asia arising from China's emission reduction strategies.

3.2. Changes in transboundary transport of air pollutants during KORUS-AQ and SIJAQ campaigns

To understand the impact of the transboundary transport of high-level pollutants comprehensively, we compared ground and aircraft measurement data with satellite images from VIIRS and MERRA-2 during the KORUS-AQ 2016; SIJAQ 2022, which were both conducted during the same spring period (May 1–June 12). Several sensitivity tests were performed in a series of steps through WRF-Chem simulations and quantitatively interpreted the effects of the emission differences between the two campaign periods.

First, to examine the overall PM concentration changes in Northeast Asia, we presented the average AOD spatial distribution from the VIIRS satellite data, MERRA-2 reanalysis data and column-integrated $PM_{2.5}$ concentrations from the WRF-Chem results (Fig. 4). Despite the model limitations, such as the exclusion of yellow dust events, the WRF-Chem simulations over East China captured well the high AOD spatial distributions shown in the satellite and reanalysis data. Both the regional chemical transport model simulation and satellite AOD data indicated a substantial decrease in PM concentrations across Northeast Asia in 2022 compared with 2016. These simulations and satellite measurements of AOD spatial distributions align well with the decrease in the bottom-up emissions depicted in Fig. 3 from 2016 to 2022. Therefore, the numerically simulated decline in PM concentrations could be strongly related to the reduced anthropogenic emissions in Northeast Asia.

The variations in air pollutants and the transboundary transport process are linked to changes in meteorological conditions in addition to emission reduction. Chemical transport models are widely used to separate changes in emissions and meteorological conditions as causes of variations in air pollutants (Ma et al., 2019; Yin et al., 2021; Wang et al., 2022). As a next step, we used WRF-Chem and exchanged meteorological conditions between two campaign periods to assess the variances influenced by meteorological factors conducive to the transboundary transport events over each period. Figs. S1–(a) shows the horizontal wind speed/direction from ground level to 800 hPa over the Yellow Sea (126°–127° E, 35°–37° N) for both campaign periods. In both periods, frequent westerly winds were found over the Yellow Sea in both the upper and lower atmospheres; in particular, westerly periods prevailed on May 25–26 and May 30–31, 2016 (Figs. S1–(a)), which were identified as typical transboundary transport cases in previous studies (Kim et al., 2017; Kim et al., 2023a). Compared with the KORUS-AQ 2016, the SIJAQ 2022 showed more frequent westerly winds directed toward Seoul. For example, vertical westerly structures, such as westerly winds from the surface to 850 hPa, lasted 42 days, unlike the 28 days during the KORUS-AQ 2016 (Figs. S1–(a)). Hence, the meteorological occurrence frequencies conducive to transboundary transport were relatively higher during the SIJAQ 2022 compared with the KORUS-AQ 2016 from the meteorological perspective. In addition, Figs. S1–(b) shows the hourly precipitation in Seoul during the two campaign periods, indicating that both the frequency and total amount of precipitation were lower during SIJAQ 2022 compared to KORUS-AQ 2016. This suggests that the SIJAQ 2022 period experienced relatively less wet deposition of PM, which likely contributed to higher $PM_{2.5}$ concentrations. High relative humidity can also influence the hygroscopic growth of PM, potentially leading to increased PM concentrations in marine areas like Baengnyeong Island. However, as shown in Fig. S1, the relative humidity levels during both campaigns, excluding precipitation days related to wet scavenging over the Yellow Sea, were similar.

To interpret the effects of emission reduction in association with various daily meteorological conditions, we examined the time series of ground measurements in Seoul. Fig. S2 shows the simulated and observed variations in the surface $PM_{2.5}$ mass and its chemical components in Seoul during the two campaign periods. As depicted in Fig. S2, ground-level $PM_{2.5}$ concentrations were generally lower during the SIJAQ 2022 compared with the KORUS-AQ 2016. For example, the highest concentration during the SIJAQ 2022 (~60 μg/m^3) was markedly lower than that during the KORUS-AQ 2016 (~90 μg/m^3) (Fig. S2). On May 24–27, 2016, May 30–June 1, 2016, May 17–19, 2022, and May 22–23, 2022, Seoul and Baengnyeong Island showed concurrent increases in $PM_{2.5}$ concentrations (Fig. S3). These periods matched the prevalence of westerly winds in the synoptic weather analysis over the

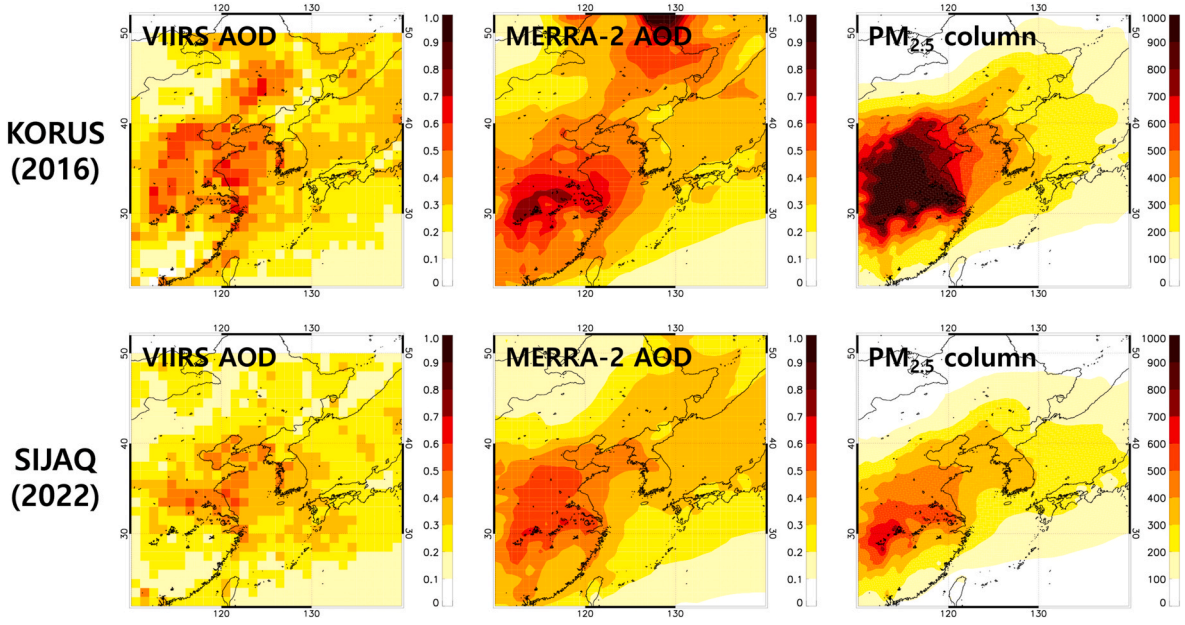


Fig. 4. Spatial distributions of AOD in VIIRS, MERRA-2 reanalysis data and column-integrated $PM_{2.5}$ concentrations in WRF-Chem results during SIJAQ 2022; KORUS-AQ 2016 campaigns.

Yellow Sea. This is indicating that the increases in observed $PM_{2.5}$ concentrations during these periods could lead to high $PM_{2.5}$ episodes resulting from the transboundary transport of China's air pollutants. Despite the frequent westerly winds with high possibility of transboundary transport episodes during the SIJAQ 2022, the Seoul measurements during this period exhibited lower $PM_{2.5}$ levels than those recorded during KORUS-AQ 2016. This suggested a decrease in air pollutants transported from East China to the Korean Peninsula in the spring of 2022.

To separate quantitatively the roles of emission changes from meteorological conditions, we further conducted WRF-Chem sensitivity experiments for the periods of 2016 and 2022. In these modeling experiments, we used emissions data from the SIJAQ 2022 and the KORUS-AQ 2016 while fixing the simulation period of the SIJAQ campaign, as designed in Table 1. Fig. 5 illustrates the spatial distribution of simulated $PM_{2.5}$ concentration differences between the SIJAQ 2022 emissions + meteorological condition (2022) and the KORUS-AQ 2016 emissions + meteorological condition (2016), as well as the results of sensitivity experiments varying emissions and meteorological conditions. Fig. 5-(c) and (d) depict the changes in $PM_{2.5}$ concentrations in Northeast Asia solely due to anthropogenic emission changes; (e) and (f) indicate the variabilities arising from meteorological differences.

First, examining the differences in meteorological conditions shown in Fig. 5-(e) and (f) reveals that model simulations using the 2022 meteorological field, compared to those from 2016, suggest a decreasing trend in $PM_{2.5}$ concentrations over the East China region. In 2016, the El Niño was in a decay phase (Peterson et al., 2019; KMA, 2016), while 2022 was characterized by persistent weak La Niña conditions (KMA, 2022). These differing climate conditions likely contributed to the observed/simulated variations in $PM_{2.5}$ concentrations. Specifically, the higher precipitation during the KORUS-AQ 2016 campaign, compared to the SIJAQ 2022 period, may have been influenced by the El Niño-Southern Oscillation (ENSO). According to Wang et al. (2023) and Qiu et al. (2017), El Niño periods typically exhibit increased precipitation, reduced solar radiation, and lower planetary boundary layer height (PBLH), while La Niña periods are associated with lower precipitation (and potentially drought), increased solar radiation, and higher PBLH. Additionally, Zhu et al. (2021) reported that spring Aerosol Optical Depth (AOD) can fluctuate depending on ENSO conditions. These meteorological variations related to ENSO can also impact on $PM_{2.5}$ concentrations.

We highlight the pronounced difference in $PM_{2.5}$ described in Fig. 5-(c) and (d), indicating that the reduction in emissions between the two periods plays a more significant role in the variation of $PM_{2.5}$ concentrations than the differences caused by meteorological conditions. According to Figs. S4 and S5 the emission reduction decreased the averaged surface $PM_{2.5}$ concentration by approximately 9.12 $\mu g/m^3$ (34.5%) in China's BTH region; a reduction of 7.53 $\mu g/m^3$ (28.3%) was simulated in Seoul, South Korea; and an approximately 4.73 $\mu g/m^3$ (23.8%) decrease was observed on Baengnyeong Island, in the Yellow Sea. Notably, Fig. S6 also reveals decreases in not only surface $PM_{2.5}$ concentrations but also column-integrated $PM_{2.5}$ concentrations across the East China region and the Korean Peninsula. Long-range-transported pollutants tend to move to downwind regions, which mostly occurs through the upper atmosphere, primarily above the atmospheric boundary layer height (Kim et al., 2018; Lee et al., 2019b). Therefore, the decline in column-integrated $PM_{2.5}$ concentrations (Fig. S6), which was larger than that in the surface concentrations over the Yellow Sea (where column-integrated and surface-level $PM_{2.5}$ concentrations were reduced by 28% and 12%, respectively), indicated a larger reduction in the mass concentrations of the long-range-transported pollutants than that in the surface $PM_{2.5}$ concentrations over the Korean Peninsula.

Table 1
Simulation scenarios for WRF-Chem model sensitivity tests in determining roles of emission changes and meteorological conditions.

Experiment	Simulation period (meteorological condition)	Emission
EXP1	May–June 2016	KORUSv5 (KORUS-AQ, 2016)
EXP2	May–June 2022	Updated CREATEv3 (SIJAQ 2022)
EXP3	May–June 2022	KORUSv5 (KORUS-AQ, 2016)
EXP4	May–June 2016	Updated CREATEv3 (SIJAQ 2022)

3.3. Changes in secondary formation processes during long-range transport

We analyzed the behavior of long-range-transported PM by considering two key processes: (1) PM transformed from gas-phase air pollutants over source regions and (2) PM transformed during transboundary transport toward downwind areas.

Fig. 6 shows the vertical distributions of the simulated and measured concentrations of air pollutants (SO_4^{2-}, NO_3^-, SO_2, and NO_2) obtained from the WRF-Chem base case modeling and aircraft measurement for the western Seoul Metropolitan Area (126.0°–127.5° E, 36.0°–38.0° N). The simulations captured the high gaseous SO_2 and NO_2 concentrations near the surface, which rapidly decreased with an increase in altitude. By contrast, for SO_4^{2-} and NO_3^-, both measurement and simulations indicated higher concentrations than those of the gaseous components, extending from the surface up to approximately 2 km in altitude. The high concentrations of SO_4^{2-} and NO_3^- at altitudes of 1–2 km could be influenced by secondary formation, vertical mixing, and the long-range transport of PM at this altitude(Zhang et al., 2009; Jeon et al., 2018; Jo et al., 2019; Lee et al., 2019a). Additionally, the comparison of simulated vertical profiles for the KORUS-AQ and SIJAQ periods revealed an overall decrease in the concentration of all species from the ground up to 3 km during the SIJAQ 2022 period compared to the KORUS-AQ period.

Due to a lack of some measured components, the comparison of vertical distributions between the KORUS-AQ 2016; SIJAQ 2022 was limited to gaseous NO_2. Since the SIJAQ 2022 campaign primarily measured concentrations below 1 km, the comparison between measurements and model results was confined to the lower atmosphere. The vertical profiles of NO_2 concentrations exhibited no substantial differences between the two periods. This analysis also demonstrated that the WRF-Chem model accurately captured both the quantitative NO_2 concentration levels and the qualitative vertical distribution patterns during the SIJAQ 2022 period. Furthermore, the simulated vertical distribution of NO_2, SO_2, SO_4^{2-}, and NO_3^- concentrations during the KORUS-AQ period closely reproduced both the average concentration levels and the overall vertical profiles from the surface up to an altitude of 3 km. The correlation coefficient (R) and Index of Agreement (IOA) between the model results and aircraft measurements indicate strong agreement with values of 0.7 or higher for most chemical species, with the exception of NO_3^-, which shows an R value of approximately 0.6 (Table S2).

Additionally, Fig. S9 assesses the model performance by comparing simulated surface concentrations of NO_3^- and SO_4^{2-} with observations measured at Olympic Park during the KORUS-AQ 2016; SIJAQ 2022 campaigns. The comparison of average concentrations from 2016 to 2022 reveals decreases of 1.6 $\mu g/m^3$ for both NO_3^- and SO_4^{2-}. These results, together with the vertical profiles of SO_4^{2-} and NO_3^- presented in Fig. 6, suggest that both sulfate and nitrate decreased from the ground up to 3 km in the atmosphere between 2016 and 2022.

Using the results of the sensitivity tests, we derived the gas-to-particle (G/P) partitioning ratio (hereinafter G/P-ratio) of inorganic aerosols and compared the oxidation capacities between the two campaign periods. Fig. 7 displays the vertical distributions of the G/P ratios averaged by latitude for 35–38° N over China, the Yellow Sea, and the Korean Peninsula, as well as the G/P ratio values for specific locations such as Beijing, Baengnyeong Island, and Seoul during the two

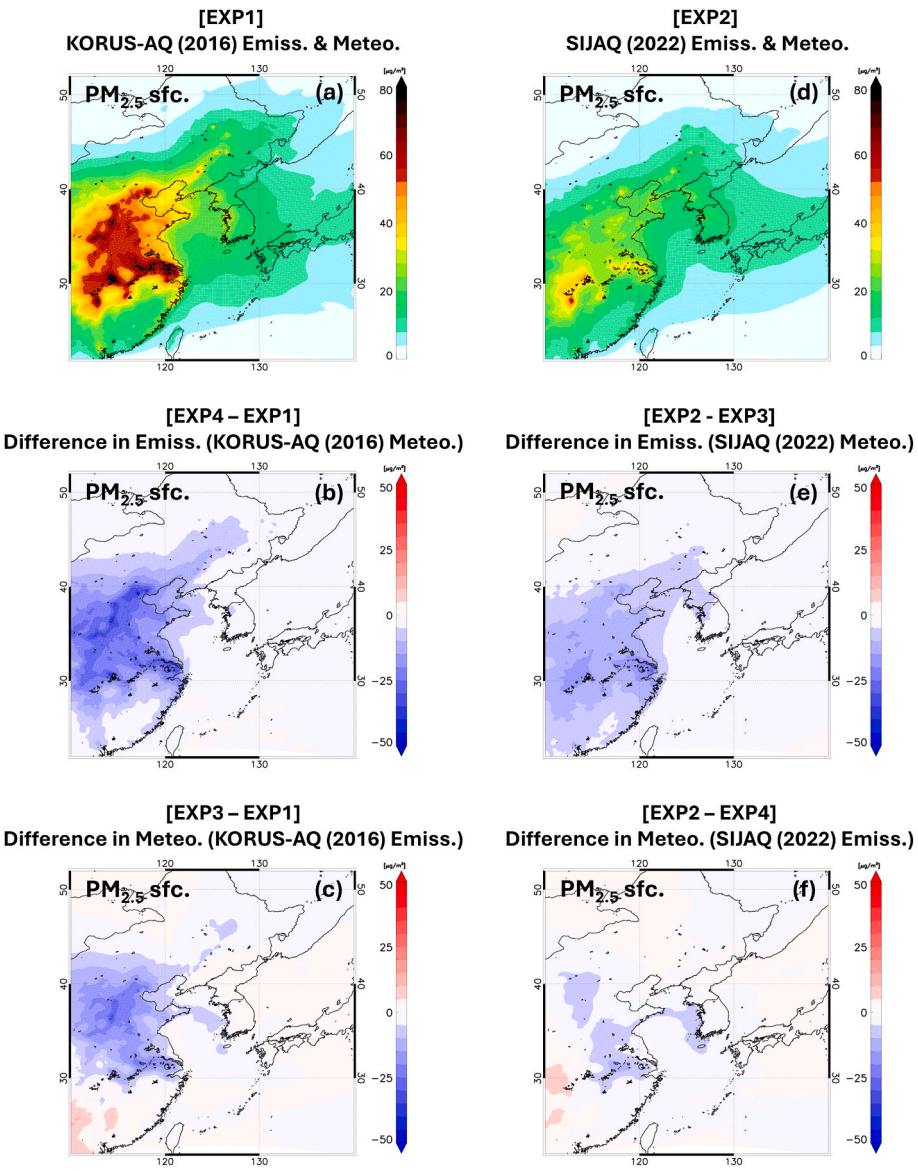


Fig. 5. Simulated spatial distributions of surface $PM_{2.5}$ concentrations from WRF-Chem modeling results during the (a) KORUS-AQ 2016 and (b) SIJAQ 2022 campaign periods. Spatial distributions of differences in surface $PM_{2.5}$ concentrations from four sensitivity tests (Table 1) based on changes in emissions (c, d) and meteorological conditions (e, f).

periods. As indicated in Fig. 7, G/P ratios of 0.8 or higher were observed at 850–700 hPa levels across East China and the Yellow Sea during KORUS-AQ 2016. However, during the SIJAQ 2022, these G/P ratios appeared in the eastern Yellow Sea and western coastal area of the Korean Peninsula, indicating that G/P conversion slowed down in East China during the SIJAQ 2022. This shift in the high-G/P-ratio region from East China/Yellow Sea toward near the Korean Peninsula reflected relatively lower secondary PM formation from the KORUS-AQ 2016 to the SIJAQ 2022. This carried more gas-phase air pollutants and smaller amounts of PM during transboundary transport in Northeast Asia.

In the lower atmosphere, overall, our findings indicated larger decreases in the G/P ratios near the surface in East China and the Yellow Sea during the SIJAQ 2022 than in the KORUS-AQ 2016 (Fig. 7a). The correlation of the G/P ratios over the Yellow Sea between the two periods (Fig. 7b) from the surface to the 700 hPa level (~3 km altitude) ranged from 0.65 to 0.90 during the KORUS-AQ and from 0.65 to 0.85 during the SIJAQ 2022. The maximum G/P-ratio also decreased by approximately 5% in this study. Thus, the reductions in precursors, such as NO_2 and SO_2, contributed to the decline in G/P ratios over the Yellow Sea.

Lastly, we analyzed the pollutant concentration variations arising from the differences in meteorological conditions between the two campaign periods. In previous studies, 3D chemical transport models were used to decouple emission effects on air pollutants from the effects of meteorological conditions, or vice versa (Shi et al., 2021; Hou et al., 2022). As seen in Table 1, we designed four sensitivity tests for this purpose, and we compared the simulated vertical distributions of aerosol and gaseous concentrations over the region from East China to the Korean Peninsula.

In addition, the impact of meteorological variations between the two campaign periods were assessed in Northeast Asia. Fig. 8 shows one example: SO_4^{2-} and gaseous SO_2 from each sensitivity test; the results for the other species are in the supplementary files. As illustrated in Fig. 8, we found significant differences in SO_4^{2-} and SO_2 concentrations between the two campaign periods (EXP1 and EXP2), particularly over East China and over the Yellow Sea. However, examining some meteorological variations (EXP1 vs. EXP3, which pertained to KORUS-AQ (2016) emissions under the same meteorological conditions), we

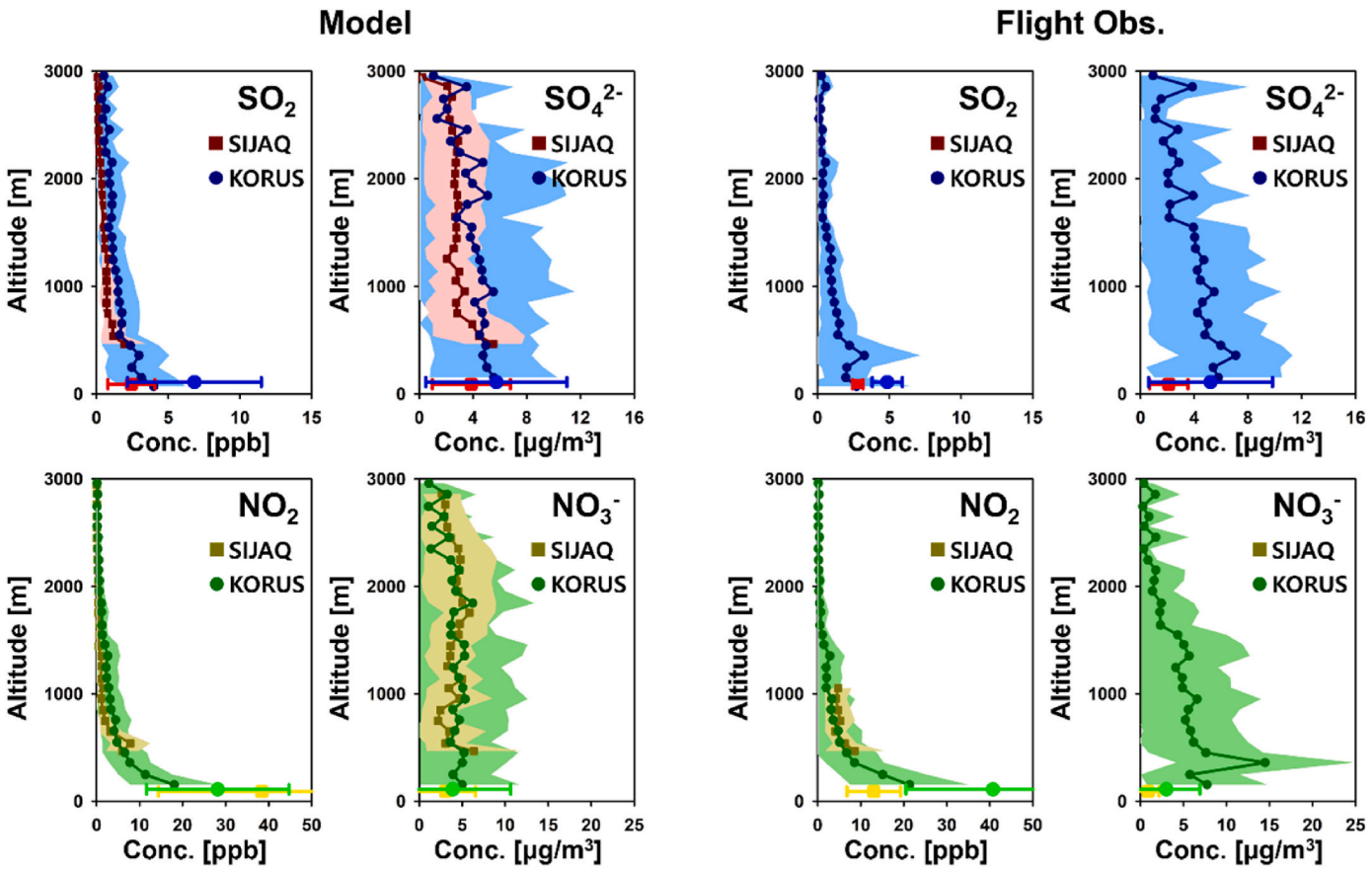


Fig. 6. Vertical distributions of SO_2, sulfate, NO_2, and NO_3^- in Seoul Metropolitan Area simulated via WRF-Chem (left) during SIJAQ 2022; KORUS-AQ 2016 campaign periods compared with aircraft measurement data (right). Large dots with error bars near the surface represent the measured and simulated concentrations at Olympic Park in Seoul.

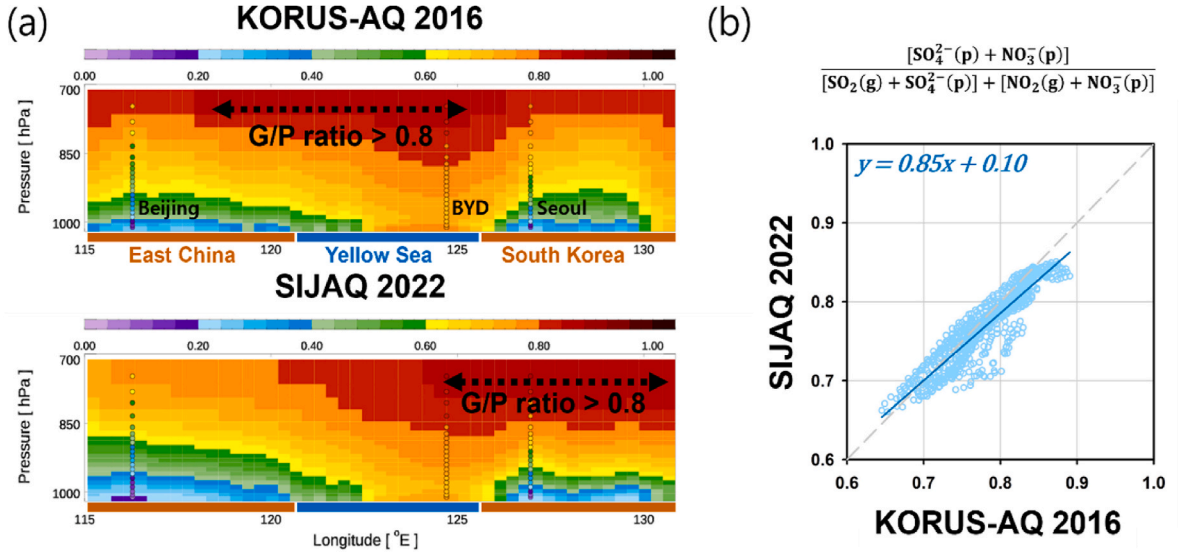


Fig. 7. (a) Distributions of secondary formation ratios averaged by latitude for 35–38° N during the SIJAQ 2022; KORUS-AQ 2016 campaign periods. Each dot represents the gas-to-particle ratios for Beijing, Baengnyeong Island, and Seoul. (b) Scatter plot of gas-to-particle conversion ratios for both campaign periods over the Yellow Sea (123.5°–124.5° E). (For interpretation of the references to colour in this figure legend, the reader is referred to the Web version of this article.)

found no noticeable differences (Fig. 8a and c). Nevertheless, small but detectable effects were simulated; EXP3 showed slightly higher results in the Korean Peninsula but marginally lower results in East China compared with EXP1 (Fig. 8). This also applied to the EXP2-versus-EXP4 comparison (Fig. 8b and d). Therefore, although only two campaign periods were tested in our study, the effect of meteorological variations showed no significant fluctuations with less than 10% in this study.

In summary, our results suggested the significant interannual

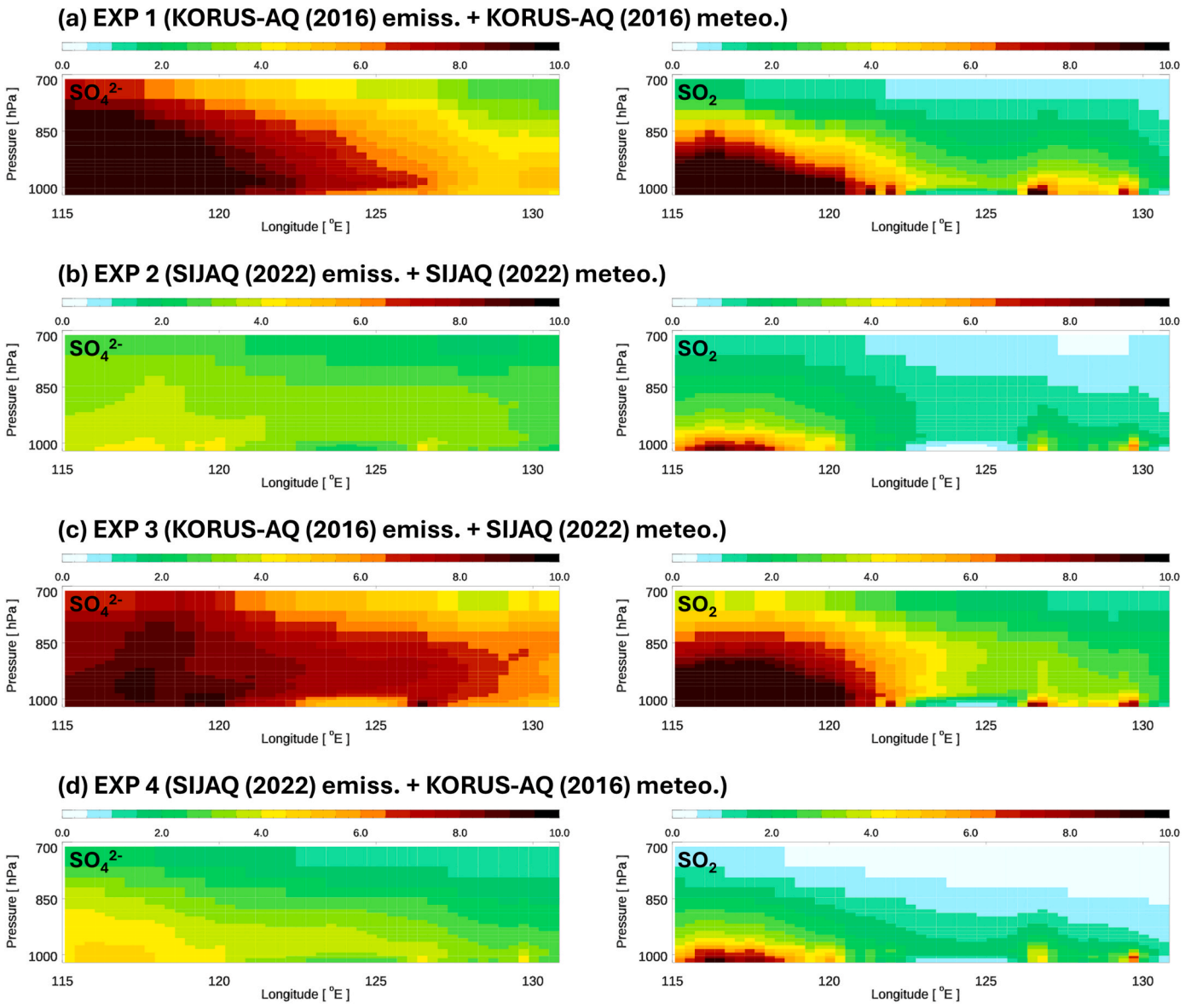


Fig. 8. Simulated vertical distributions of SO_4^{2-} and its gas-phase precursor SO_2 concentrations from four sensitivity tests (Table 1) over Northeast Asia across region spanning East China, Yellow Sea, and Korean Peninsula: (a) KORUS-AQ 2016 emissions and KORUS-AQ 2016 meteorological condition; (b) SIJAQ 2022 emissions and SIJAQ 2022 meteorological condition; (c) KORUS-AQ 2016 emissions and SIJAQ 2022 meteorological condition; (d) SIJAQ 2022 emissions and KORUS-AQ 2016 meteorological condition. (For interpretation of the references to colour in this figure legend, the reader is referred to the Web version of this article.)

variations with improvements in air quality, particularly $PM_{2.5}$ over the period from 2016 (KORUS-AQ, 2016) to 2022 (SIJAQ 2022), and the primary drivers of the interannual variations between years were emission reductions in most source areas, rather than meteorological variability in Northeast Asia.

4. Conclusion

To assess the effectiveness of ongoing air pollution reduction policies in Northeast Asia, we analyzed air quality trends in high-emission regions, specifically East China (BTH region) and the Korean Peninsula. Our study focused on two campaign periods: KORUS-AQ 2016; SIJAQ 2022, utilizing ground, satellite, and aircraft measurements from these extensive campaigns. Additionally, sensitivity experiments using WRF-Chem model were conducted for both periods to evaluate recent interannual changes in air quality over Northeast Asia.

Our findings indicate that from 2016 to 2022, air quality improvements over the Korean Peninsula were influenced by reduced emissions not only in South Korea but also in the upwind region of China. We observed significant reductions in SO_2 and NO_3, as well as in particulate SO_4^{2-} and NO_3^- in both lower and upper atmospheres during SIJAQ 2022 compared to KORUS-AQ 2016. Notably, SO_2 and $PM_{2.5}$ concentrations decreased significantly in East China, and the rate of PM secondary formation through chemical reactions in the Yellow Sea also declined. High G/P ratios shifted slightly eastward over the Yellow Sea (towards the western coastal area of the Korean Peninsula), with reduced transboundary PM due to slower G/P conversion. This suggests that air pollution reduction policies in source regions have been a major factor in improving air quality across Northeast Asia. The decrease in primary pollutants in these regions has led to lower secondary pollutants during transboundary transport, contributing to improved air quality in downwind areas.

We also examined the impact of meteorological conditions through WRF-Chem sensitivity simulations and evaluated their influence on air quality changes in Northeast Asia. Although climatic and meteorological factors, such as ENSO, also affect air quality, our results strongly

indicate that emission reductions in main source regions have significantly lowered levels of both PM and its precursors, such as SO_2 and NO_2, across Northeast Asia. Specifically, the reduction in anthropogenic emissions was the primary driver of improved air quality, with secondary contributions from changes in $PM_{2.5}$ formation during transboundary transport also being significant.

Future studies should consider long-term climate variations and conduct comprehensive model sensitivity experiments over extended periods to assess changes in air quality resulting from decade-long emission reductions. Nonetheless, our inter-annual results, derived from analyzing correlations between the two campaign periods and exploring secondary chemical transformations during transboundary transport, are expected to be valuable for shaping future pollution reduction policies in downwind regions.

CRediT authorship contribution statement

Min-Jun Park: Writing – original draft, Visualization, Validation, Methodology, Investigation, Data curation, Conceptualization. **Seung-Hee Baek:** Visualization, Validation, Investigation. **Hyo-Jung Lee:** Writing – review & editing, Supervision, Methodology, Investigation, Conceptualization. **Hyun-Young Jo:** Writing – review & editing, Supervision, Investigation. **Cheol-Hee Kim:** Writing – review & editing, Project administration. **Jin-Seok Kim:** Resources, Data curation. **Jung-Hun Woo:** Methodology, Investigation. **Rokjin Park:** Methodology, Investigation. **Jong-Jae Lee:** Validation, Data curation. **Chang-Keun Song:** Methodology, Investigation. **Jung-Woo Yoo:** Software, Data curation. **Lim-Seok Chang:** Methodology, Data curation. **Taehyoung Lee:** Methodology, Data curation.

Funding

This research was supported by the Basic Science Research Program through the National Research Foundation of Korea (NRF), funded by the Ministry of Education (NRF-2020R1A6A1A03044834) and the Korean Government (MSIT) (NRF-2022R1A2C1008132).

Declaration of competing interest

The authors declare that they have no known competing financial interests or personal relationships that could have appeared to influence the work reported in this paper.

Appendix A. Supplementary data

Supplementary data to this article can be found online at https://doi.org/10.1016/j.envpol.2024.125114.

Data availability

All modeling and measured data related to this paper are available from the corresponding author on reasonable request.

References

Chen, Z., Chen, D., Kwan, M.-P., Chen, B., Gao, B., Zhuang, Y., Li, R., Xu, B., 2019. The control of anthropogenic emissions contributed to 80% of the decrease in PM2.5 concentrations in Beijing from 2013 to 2017. Atmos. Chem. Phys. 19, 13519–13533. https://doi.org/10.5194/acp-19-13519-2019.

Cheng, L., Wei, W., Cheng, S., Zhang, C., Ye, Z., Wang, K., Wang, R., 2024. Reductions of multiple air pollutants from coking industry through technology improvements and their impacts on air quality and health risks in a highly industrialized region of China. Sci. Total Environ. 908, 168360. https://doi.org/10.1016/j.scitotenv.2023.168360.

Crawford, J.H., Ahn, J.-Y., Al-Saadi, J., Chang, L., Emmons, L.K., Kim, J., Lee, G., Park, J.-H., Park, R.J., Woo, J.H., Song, C.-K., Hong, J.-H., Hong, Y.-D., Lefer, B.L., Lee, M., Lee, T., Kim, S., Min, K.-E., Yum, S.S., Shin, H.J., Kim, Y.-W., Choi, J.-S., Park, J.-S., Szykman, J.J., Long, R.W., Jordan, C.E., Simpson, I.J., Fried, A., Dibb, J. E., Cho, S.Y., Kim, Y.P., 2021. The Korea–United States air quality (KORUS-AQ) field study. Elem. Sci. Anth. 9 (1), 00163. https://doi.org/10.1525/elementa.2020.00163.

Feng, Y., Ning, M., Lei, Y., Sun, Y., Liu, W., Wang, J., 2019. Defending blue sky in China: effectiveness of the "air pollution prevention and control action plan" on air quality improvements from 2013 to 2017. J. Environ. Manag. 252, 109603. https://doi.org/10.1016/j.jenvman.2019.109603.

Fuzzi, S., Baltensperger, U., Carslaw, K., Decesari, S., Denier van der Gon, H., Facchini, M.C., Fowler, D., Koren, I., Langford, B., Lohmann, U., Nemitz, E., Pandis, S., Riipinen, I., Rudich, Y., Schaap, M., Slowik, G.J., Spracklen, D.V., Vignati, E., Wild, M., Williams, M., Gilardoni, S., 2015. Particulate matter, air quality and climate: lessons learned and future needs. Atmos. Chem. Phys. 15, 8217–8299. https://doi.org/10.5194/acp-15-8217-2015.

Gao, M., Liu, Z., Zheng, B., Ji, D., Sherman, P., Song, S., Xin, J., Liu, C., Wang, Y., Zhang, Q., Xing, J., Jiang, J., Wang, Z., Carmichael, G.R., McElroy, M.B., 2020. China's emission control strategies have suppressed unfavorable influences of climate on wintertime $PM_{2.5}$ concentrations in Beijing since 2002. Atmos. Chem. Phys. 20, 1497–1505. https://doi.org/10.5194/acp-20-1497-2020.

Gelaro, R., McCarty, W., Suarez, M.J., Todling, R., Molod, A., Takacs, L., Randles, C., Darmenov, A., Bosilovich, M.G., Reichle, R., Wargan, K., Coy, L., Cullather, R., Draper, C., Akella, S., Buchard, V., Conaty, A., da Silva, A., Gu, W., Kim, G.-K., Koster, R., Lucchesi, R., Merkova, D., Nielsen, J.E., Partyka, G., Pawson, S., Putman, W., Rienecker, M., Schubert, S.D., Sienkiewicz, M., Zhao, B., 2017. The Modern-era retrospective analysis for research and applications, version 2 (MERRA-2). J. Clim. 30, 5419–5454. https://doi.org/10.1175/JCLI-D-16-0758.1.

Grell, G.A., Peckham, S.E., Schmitz, R., McKeen, S.A., Frost, G., Skamarock, W.C., Eder, B., 2005. Fully coupled "online" chemistry within the WRF model. Atmos. Environ. 39, 6957–6975. https://doi.org/10.1016/j.atmosenv.2005.04.027.

Guo, J., He, J., Liu, H., Miao, Y., Liu, H., Zhai, P., 2016. Impact of various emission control schemes on air quality using WRF-Chem during APEC China 2014. Atmos. Environ. 140, 311–319. https://doi.org/10.1016/j.atmosenv.2016.05.046.

Hamamoto, M., 2006. Environmental regulation and the productivity of Japanese manufacturing industries. Resour. Energy Econ. 28 (4), 299–312. https://doi.org/10.1016/j.reseneeco.2005.11.001.

Han, X., Cai, J., Zhang, M., Wang, X., 2021. Numerical simulation of interannual variation in transboundary contributions from Chinese emissions to PM2.5 mass burden in South Korea. Atmos. Environ. 256, 118440. https://doi.org/10.1016/j.atmosenv.2021.118440.

He, M., Ichinose, T., Yoshida, Y., Arashidani, K., Yoshida, S., Takano, H., Sun, G., Shibamoto, T., 2017. Urban PM2.5 exacerbates allergic inflammation in the murine lung via a TLR2/TLR4/MyD88-signaling pathway. Sci. Rep. 7, 11027. https://doi.org/10.1038/s41598-017-11471-y.

Hou, L., Dai, Q., Song, C., Liu, B., Guo, F., Dai, T., Li, L., Liu, B., Bi, X., Zhang, Y., Feng, Y., 2022. Revealing drivers of haze pollution by explainable machine learning. Environ. Sci. Technol. Lett. 9, 112–119. https://doi.org/10.1021/acs.estlett.1c00865.

Itawa, K., Arimura, T.H., Shimane, T., 2014. The effectiveness of vehicle emission control policies: evidence from Japanese experience. Tokyo Center for Economic Research. Paper No. E-77, https://ssrn.com/abstract=2438618.

Jeon, W., Choi, Y., Mun, J., Lee, S.-H., Choi, H.-J., Yoo, J.-W., Lee, H.-J., Lee, H.-W., 2018. Behavior of sulfate on the sea surface during its transport from Eastern China to South Korea. Atmos. Environ. 186, 102–112. https://doi.org/10.1016/j.atmosenv.2018.05.017.

Jo, H.-Y., Lee, H.-J., Jo, Y.-J., Lee, J.-J., Ban, S., Lee, J.J., Chang, L.S., Heo, G., Kim, C.H., 2019. Nocturnal fine particulate nitrate formation by N2O5 heterogeneous chemistry in Seoul Metropolitan Area, Korea. Atmos. Res. 225, 58–69. https://doi.org/10.1016/j.atmosres.2019.03.028.

Jo, H.-Y., Lee, H.-J., Jo, Y.-J., Heo, G.-Y., Lee, M.-H., Kim, J.-A., Park, M.-S., Lee, T.-H., Kim, S.-W., Lee, Y.-H., Kim, C.-H., 2022. A case study of heavy $PM_{2.5}$ secondary formation by N_2O_5 nocturnal chemistry in Seoul, Korea in January 2018: model performance and error analysis. Atmos. Res. 266, 105951. https://doi.org/10.1016/j.atmosres.2021.105951.

Jo, Y.-J., Lee, H.-J., Jo, H.-Y., Woo, J.-H., Kim, Y.-H., Lee, T.-H., Heo, G.-Y., Park, S.-M., Jung, D.-H., Park, J.-H., Kim, C.-H., 2020. Changes in inorganic aerosol compositions over the Yellow Sea area from impact of Chinese emissions mitigation. Atmos. Res. 240, 104948. https://doi.org/10.1016/j.atmosres.2020.104948.

Kaneyasu, N., Yamamoto, S., Sato, K., Takami, A., Hayashi, M., Hara, K., Kawamoto, K., Okuda, T., Hatakeyama, S., 2014. Impact of long-range transport of aerosols on the $PM_{2.5}$ composition at a major metropolitan area in the northern Kyushu area of Japan. Atmos. Environ. 97, 416–425. https://doi.org/10.1016/j.atmosenv.2014.01.029.

Kim, C.-H., Jo, H.-Y., Jo, Y.-J., Lee, H.-J., Kim, J.-M., Lee, N.-M., Jeong, S.-Y., Baek, S.-H., Park, M.-J., Chang, L.-S., Lee, J.-J., Song, C.-K., 2023a. Synoptic meteorological conditions and contributing factors to air quality during the SIJAQ campaign. Atmos. Environ. 309, 119939. https://doi.org/10.1016/j.atmosenv.2023.119939.

Kim, H.-C., Kim, S.-T., Kim, B.-U., Jin, C.-S., Hong, S.-Y., Park, R.-J., Son, S.-W., Bae, C.-H., Bae, M.-A., Song, C.-K., Stein, A., 2017. Recent increase of surface particulate matter concentrations in the Seoul Metropolitan Area, Korea. Sci. Rep. 7, 4710. https://doi.org/10.1038/s41598-017-05092-8.

Kim, H.-J., Zhang, Q., Heo, J.-B., 2018. Influence of intense secondary aerosol formation and long-range transport on aerosol chemistry and properties in the Seoul Metropolitan Area during spring time: results from KORUS-AQ. Atmos. Chem. Phys. 18, 7149–7168. https://doi.org/10.5194/acp-18-7149-2018.

Kim, S.Y., Kim, J.S., Hu, H.J., Jang, M.D., Lee, J.B., Hong, S.C., Kim, O.K., Woo, J.H., 2023b. Update of the year 2019 modeling emissions inventory in China. Asian J. Atmos. Environ. 17 (20). https://doi.org/10.1007/s44273-023-00012-x.

Kim, Y.P., Lee, G.W., 2018. Trend of air quality in Seoul: policy and science. Aerosol Air Qual. Res. 18, 2141–2156. https://doi.org/10.4209/aaqr.2018.03.0081.

KMA, 2016. Annual climatological report 2016. 11-1360000-000016-10. https://data.kma.go.kr/data/publication/publicationAsosList.do?pgmNo=143.
KMA, 2022. Annual climatological report 2022. 11-1360000-000016-10. https://data.kma.go.kr/data/publication/publicationAsosList.do?pgmNo=143.
Lee, H.J., Jo, H.Y., Park, S.Y., Jo, Y.J., Jeon, W.B., Ahn, J.Y., Kim, C.H., 2019a. A case study of the transport/transformation of air pollutants over the Yellow Sea during the MAPS 2015 campaign. J. Geophys. Res. Atmos. 124, 6532–6553. https://doi.org/10.1029/2018JD029751.
Lee, H.J., Jo, H.Y., Kim, S.W., Park, M.S., Kim, C.H., 2019b. Impacts of atmospheric vertical structures on transboundary aerosol transport from China to South Korea. Sci. Rep. 9, 13040. https://doi.org/10.1038/s41598-019-49691-z.
Lee, H.J., Chang, I.S., Jaffe, D.A., Bak, J., Liu, X., Abad, G.G., Jo, H.Y., Jo, Y.J., Lee, J.B., Kim, C.H., 2021. Ozone continues to increase in East Asia despite decreasing NO2: causes and abatements. Rem. Sens. 13, 2177. https://doi.org/10.3390/rs13112177.
Lee, H.J., Jo, Y.J., Kim, S., Kim, D., Kim, J.M., Choi, D., Jo, H.Y., Bak, J., Park, S.Y., Jeon, W., Kim, C.H., 2022. Transboundary aerosol transport process and its impact on aerosol-radiation-cloud feedbacks in springtime over Northeast Asia. Sci. Rep. 12, 4870. https://doi.org/10.1038/s41598-022-08854-1.
Lee, H.J., Jo, H.Y., Kim, J.M., Bak, J., Park, M.S., Kim, J.W., Jo, Y.J., Kim, C.H., 2023. Nocturnal boundary layer height uncertainty in particulate matter simulations during the KORUS-AQ campaign. Rem. Sens. 15, 300. https://doi.org/10.3390/rs15020300.
Liu, X.J., Xu, W., Du, E.Z., Tang, A.H., Zhang, Y., Zhang, Y.Y., Wen, Z., Hao, T.X., Pan, Y. P., Zhang, L., Gu, B.J., Zhao, Y., Shen, J.L., Zhou, F., Gao, Z.L., Feng, Z.Z., Chang, Y. H., Goulding, K., Collett Jr, J.L., Vitousek, P.M., Zhang, F.S., 2020. Environmental impacts of nitrogen emissions in China and the role of policies in emission reduction. Phil. Trans. R. Soc. A378, 20190324. https://doi.org/10.1098/rsta.2019.0324.
Lu, X., Zhang, S., Xing, J., Wang, Y., Chen, W., Ding, D., Wu, Y., Wang, S., Duan, L., Hao, J., 2020. Progress of air pollution control in China and its challenges and opportunities in the ecological civilization Era. Engineering 6, 1423–1431. https://doi.org/10.1016/j.eng.2020.03.014.
Ma, X., Jia, H., Sha, T., An, J., Tian, R., 2019. Spatial and seasonal characteristics of particulate matter and gaseous pollution in China: implications for control policy. Environ. Pollut. 248, 421–428. https://doi.org/10.1016/j.envpol.2019.02.038.
Matus, K., Nam, K.M., Selin, N.E., Lamsal, L.N., Reilly, J.M., Paltsev, S., 2012. Health damages from air pollution in China. Global Environ. Change 22, 55–66. https://doi.org/10.1016/j.gloenvcha.2011.08.006.
NCEP, 2000. NCEP FNL operational model global tropospheric analyses, continuing from july 1999. https://oidc.rda.ucar.edu/datasets/d083002/.
NIER, NASA, 2017. Rapid science synthesis report. In: English. Available at: https://espo.nasa.gov/sites/default/files/documents/KORUS-AQ-ENG.pdf.
Park, J., Mun, J., Kim, D., Lee, H.W., Kim, C.H., Lee, H.J., Jo, H.Y., Koo, J.H., Choe, H.S., Jeon, W., 2024. Assessing the impact of shipping emissions on ozone concentrations in East Asia: insights from KORUS-AQ and SIJAQ 2021 campaign periods. Atmos. Environ. 320, 120339. https://doi.org/10.1016/j.atmosenv.2024.120339.
Park, R.J., Oak, Y.J., Emmons, L.K., Kim, C.H., Pfister, G.G., Carmichael, G.R., Saide, P. E., Cho, S.Y., Kim, S.T., Woo, J.H., Crawford, J.H., Gaubert, B., Lee, H.J., Park, S.Y., Jo, Y.J., Gao, M., Tang, B., Stanier, C.O., Shin, S.S., Park, H.Y., Bae, C.H., Kim, E.H., 2021. Multi-model intercomparisons of air quality simulations for the KORUS-AQ campaign. Elem. Sci. Anth. 9, 1. https://doi.org/10.1525/elementa.2021.00139.
Peterson, D.A., Hyer, E.J., Han, S.O., Crawford, J.H., Park, R.J., Holz, R., Kuehn, R.E., Eloranta, E., Knote, C., Jordan, C.E., Lefer, B.L., 2019. Meteorology influencing springtime air quality, pollution transport, and visibility in Korea. Elem. Sci. Anth. 7, 57. https://doi.org/10.1525/elementa.395.
Qiu, S., Zhou, W., Leung, M.Y., Li, X., 2017. Regional moisture budget associated with drought/flood events over China. Prog. Earth Planet. Sci. 4, 36. https://doi.org/10.1186/s40645-017-0148-3.
Shi, W., Bi, J., Liu, R., Liu, M., Ma, Z., 2021. Decrease in the Chronic Health Effects from $PM_{2.5}$ during the 13th Five-Year Plan in China: Impacts of Air Pollution Control Policies, vol. 317, 128433. https://doi.org/10.1016/j.jclepro.2021.128433.
Skamarock, W.C., Klemp, J.B., 2008. A time-split nonhydrostatic atmospheric model for weather research and forecasting applications. J. Comput. Phys. 227, 3465–3485. https://doi:10.1016/j.jcp.2007.01.037.
Sun, Y., Wang, Z., Wild, O., Xu, W., Chen, C., Fu, P., Du, W., Zhou, L., Zhang, Q., Han, T., Wang, Q., Pan, X., Zheng, H., Li, J., Guo, X., Liu, J., Worsnop, D.R., 2016. "APEC Blue": secondary aerosol reductions from emission controls in Beijing. Sci. Rep. 6, 20668. https://doi.org/10.1038/srep20668.
Wang, S., Xing, J., Zhao, B., Jang, C., Hao, J., 2014. Effectiveness of national air pollution control policies on the air quality in metropolitan areas of China. J. Environ. Sci. 26, 13–22. https://doi.org/10.1016/S1001-0742(13)60381-2.
Wang, Y., Huang, C., Hu, J., Wang, M., 2022. Development of high-resolution spatio-temporal models for ambient air pollution in a metropolitan area of China from 2013 to 2019. Chemosphere 291, 132918. https://doi.org/10.1016/j.chemosphere.2021.132918.
Wang, C.Y., Chen, J.P., Wang, W.C., 2023. Meteorology-driven PM2.5 interannual variability over East Asia. Sci. Total Environ. 904, 166911. https://doi.org/10.1016/j.scitotenv.2023.166911.
WHO (World Health Organization), 2013. Health effects of particulate matter: policy implications for countries in eastern Europe, Caucasus and central Asia. https://apps.who.int/iris/h.
Woo, J.H., Kim, Y.H., Kim, H.K., Choi, K.C., Eum, J.H., Lee, J.B., Lim, J.H., Kim, J.Y., Seong, M.A., 2020. Development of the CREATE inventory in support of integrated climate and air quality modeling for Asia. Sustainability 12 (19), 7930. https://doi.org/10.3390/su12197930.
Wu, Y., Zhang, S., Hao, J., Liu, H., Wu, X., Hu, J., Walsh, M.P., Wallington, T.J., Zhang, K.M., Stevanovic, S., 2017. On-road vehicle emissions and their control in China: a review and outlook. Sci. Total Environ. 574, 332–349. https://doi.org/10.1016/j.scitotenv.2016.09.040.
Xia, Y., Zhao, Y., Nielsen, C.P., 2016. Benefits of China's efforts in gaseous pollutant control indicated by the bottom-up emissions and satellite observations 2000–2014. Atmos. Environ. 136, 43–53. https://doi.org/10.1016/j.atmosenv.2016.04.013.
Xie, P., Liao, H., 2022. The impacts of changes in anthropogenic emissions over China on PM2.5 concentrations in South Korea and Japan during 2013–2017. Front. Environ. Sci. 10, 841285. https://doi.org/10.3389/fenvs.2022.841285.
Yin, H., Lu, X., Sun, Y., Li, K., Gao, M., Zheng, B., Liu, C., 2021. Unprecedented decline in summertime surface ozone over eastern China in 2020 comparably attributable to anthropogenic emission reductions and meteorology. Environ. Res. Lett. 16, 124069. https://doi.org/10.1088/1748-9326/ac3e22.
Zeng, Y., Cao, Y., Qiao, X., Seyler, B.C., Tang, Y., 2019. Air pollution reduction in China: recent success but great challenge for the future. Sci. Total Environ. 663, 329–337. https://doi.org/10.1016/j.scitotenv.2019.01.262.
Zhang, Q., Ma, X.C., Tie, X., Huang, M., Zhao, C., 2009. Vertical distributions of aerosols under different weather conditions: analysis of in-situ aircraft measurements in Beijing, China. Atmos. Environ. 43, 5526–5535. https://doi.org/10.1016/j.atmosenv.2009.05.037.
Zhang, R., Sun, X., Shi, A., Huang, Y., Yan, J., Nie, T., Yan, X., Li, X., 2018. Secondary inorganic aerosols formation during haze episodes at an urban site in Beijing, China. Atmos. Environ. 177, 275–282. https://doi.org/10.1016/j.atmosenv.2017.12.031.
Zheng, B., Tong, D., Li, M., Liu, F., Hong, C., Geng, G., Li, H., Li, X., Peng, L., Qi, J., Yan, L., Zhang, Y., Zhao, H., Zheng, Y., He, K., Zhang, Q., 2018. Trends in China's anthropogenic emissions since 2010 as the consequences of clean air actions. Atmos. Chem. Phys. 18, 14095–14111. https://doi.org/10.5194/acp-18-14095-2018.
Zheng, Y., Xue, T., Zhao, H., Lei, Y., 2022. Increasing life expectancy in China by achieving its 2025 air quality target. Environ. Sci. Ecotech 12, 100203. https://doi.org/10.1016/j.ese.2022.100203.
Zhu, A., Xu, H., Deng, J., Ma, J., Li, S., 2021. El niño–southern oscillation (ENSO) effect on interannual variability in spring aerosols over East Asia. Atmos. Chem. Phys. 21, 5919–5933. https://doi.org/10.5194/acp-21-5919-2021.